Earth and Planetary Science Letters 420 (2015) 66–72

Contents lists available at ScienceDirect

Earth and Planetary Science Letters

www.elsevier.com/locate/epsl

Climate changes control offshore crustal structure at South China Sea continental margin

Peter D. Clift [a,*], Sascha Brune [b,c], Javier Quinteros [c]

[a] Department of Geology and Geophysics, Louisiana State University, Baton Rouge, LA 70803, USA
[b] EarthByte Group, School of Geosciences, University of Sydney, NSW 2006, Australia
[c] German Research Centre for Geosciences GFZ, 14473 Potsdam, Germany

ARTICLE INFO

Article history:
Received 6 November 2014
Received in revised form 12 March 2015
Accepted 15 March 2015
Available online xxxx
Editor: A. Yin

Keywords:
South China Sea
tectonics
extension
erosion

ABSTRACT

Rifted continental lithosphere subsides as a consequence of combined crustal thinning and mantle lithosphere cooling yet basins on some continental margins experience anomalous subsidence events that postdate active extension. Deep basins on the northern margin of the South China Sea, notably the Baiyun Sag, show basement subsidence accelerating after ~21 Ma, postdating extension by several million years. We combine geophysical observations and numerical forward modeling to show that loading of the offshore basins by increased sediment flux caused by faster onshore erosion following Early Miocene monsoon intensification is a viable trigger for ductile flow after the cessation of active extension. This illustrates that offshore basin dynamics at continental margins with weak crust can be controlled by onshore surface processes in a newly recognized form of climate–tectonic coupling.

1. Introduction

Crustal thickness in rifted continental margins largely reflects the processes of extension that are driven by plate tectonic forces. Initial crustal thicknesses are reduced by extension during continental break-up, resulting in subsidence mostly due to isostatic compensation (McKenzie, 1978). However, in certain tectonic settings significant portions of the continental crust can act in a ductile fashion (Kruse et al., 1991; Wernicke, 1990), resulting in flow away from areas of thickened crust (Clark and Royden, 2000). A flattened Moho under some extensional terrains demonstrates that flow may be important in accommodating strain and that isostatic equilibrium is not always achieved in the asthenosphere (Zuber et al., 1986). In particular, areas with higher heatflow and thicker crust tend to exhibit significant viscous mechanical behavior below the crustal brittle–ductile transition (Block and Royden, 1990; Kruse et al., 1991; Zuber et al., 1986). In this study we model the importance of ductile flow during the break-up of the South China Sea (Fig. 1), whose affected crust originally located within a Mesozoic magmatic arc that began to extend no later than the Eocene (Franke et al., 2014; Morley, 2012), and culminating in seafloor spreading around 30 Ma (Barckhausen et al., 2014; Briais et al., 1993). We show that sediment loading caused by faster erosion onshore following the onset of wetter climatic conditions can result in thinning of the crust under super-deep offshore basins after the end of tectonic extension.

2. Geological setting

The South China Sea is the largest of a series of marginal seas fringing SE and Eastern Asia and whose development has variously been ascribed to plate tectonic forces related to subduction in Indonesia and the Pacific (Morley, 2002; Taylor and Hayes, 1983) and to the relative extrusion of Indochina as a rigid block away from the India–Eurasia collision zone (Peltzer and Tapponnier, 1988). Whatever the original cause of the extension a number of sub-basins have formed on the margins of this oceanic tract and whose vertical tectonics does not follow standard models for continental extension.

Backstripping analysis has shown that the amount of subsidence observed along the northern margin of the South China Sea is much greater than that predicted from the degree of brittle upper crustal extension seen in seismic profiles (Clift et al., 2002; Davis and Kusznir, 2004). Some studies have argued that the additional subsidence is in part caused by the location of the South China Sea overlying a region of colder than normal mantle (Lithgow-Bertelloni and Gurnis, 1997), but other evidence suggests that such dynamic subsidence is <300 m in this area and cannot be responsible for short wavelength and/or rapid subsidence events (Petersen et al., 2010; Wheeler and White, 2002). If we are

* Corresponding author.
E-mail address: pclift@lsu.edu (P.D. Clift).

http://dx.doi.org/10.1016/j.epsl.2015.03.032
0012-821X/

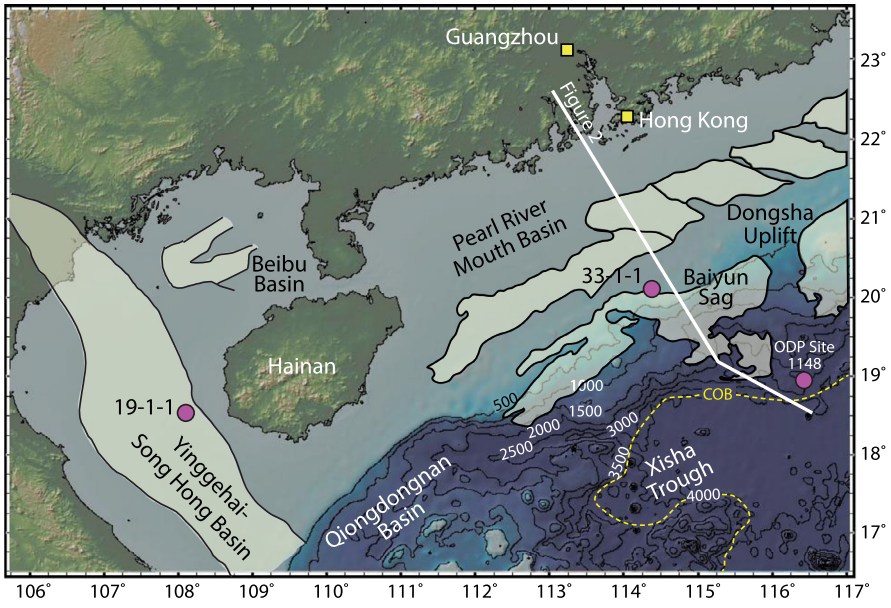

Fig. 1. Shaded bathymetric maps of the study area showing the location of features mentioned in the text. Light shaded areas show deeper areas of subsidence separated by structural highs.

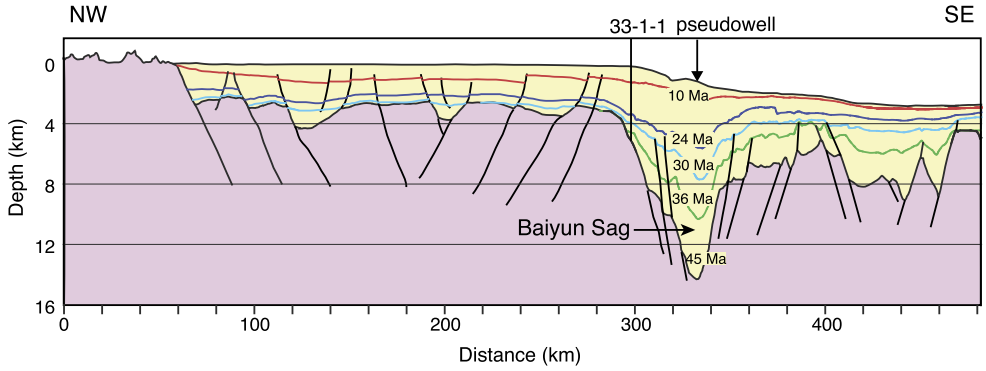

Fig. 2. Structural section across the South China margin and the Baiyun Sag compiled from Sun et al. (2008) and depth converted using drilling data from wells in the Pearl River Mouth Basin and stacking velocities from the central Baiyun Sag.

to explain the excess subsidence by crustal thinning then the extra attenuation must be assigned to the ductile part of the crust because the upper crust is well defined. Preferential lower crustal extension increases towards the continent–ocean boundary (COB) (Clift et al., 2002; Davis and Kusznir, 2004), consistent with ductile lower crustal flow from areas of thick crust towards zones of crustal thinning, as has been proposed for the Tibetan Plateau (Clark and Royden, 2000) and the rifts of the Basin and Range (Kruse et al., 1991; Zuber et al., 1986).

In order to assess the potential role of crustal flow in governing subsidence anomalies in the South China Sea we use a combination of reverse modeling of geologic data and finite element modeling to explore how post-rift subsidence can be accelerated.

3. Subsidence anomalies

A range of observations indicate anomalous subsidence at the northern continental margin of the South China Sea. In the Yinggehai–Song Hong pull-apart basin (YSHB), located to the west of Hainan Island (Fig. 1), a sharp increase in subsidence occurred at ~5 Ma (Fig. 3A) when there was very little brittle deformation (Clift and Sun, 2006). Moreover, the largest subsidence anomaly in the YSHB was spatially related to the region of fastest sedimentation, suggesting that the two might be linked. Mismatch between total subsidence and the observed degree of brittle extension is particularly noteworthy in some deep basins on the outer continental shelf, especially the Baiyun Sag (Fig. 1), where brittle faulting shows only modest degrees of horizontal extension (Sun et al., 2008; Zhao et al., 2011) (Fig. 2). In this case high degrees of crustal flow would be required to explain the total basin depths, regardless of when the extension occurred.

Analysis of tectonically driven basement motion in the Baiyun Sag accounts for sediment loading, sediment compaction and water depths of sedimentation. We applied standard backstripping methods (Sclater and Christie, 1980) to a "pseudowell" (i.e., a section which has not actually been drilled) in the center of Baiyun Sag, assuming local isostatic equilibrium in order to isolate the subsidence driven by tectonic processes. The greatest uncertainty is the assignment of palaeo-water depths of sedimentation. Modern water depths are ~1200 m in the basin center, but otherwise we follow the water depth reconstructions from a recent synthesis of drilling data (Xie et al., 2013). Well 33-1-1, which is positioned on the landward edge of the basin, is used for age control (Fig. 1; Table 1). This well is also used as a guide to lithological information, which is used to correct for the effects of sediment compaction.

Because Well 33-1-1 is located landward of the basin center we estimate that the sediment in the pseudowell would be slightly

Table 1
Age, depth and lithology data from Well 33-1-1, located at 20°5′16.7″, 114°22′21.6″ used for estimating age and lithology in the pseudowell section located in the axis of the Baiyun Sag basin.

Depth below sealevel (m)	Lithology			Water depths of sedimentation		
	Age (Ma)	Shale (%)	Siltstone (%)	Sandstone (%)	Maximum (m)	Minimum (m)
Panyu 33-1-1						
216	0	40	40	20	188	188
1029	5.5	40	40	20	200	75
1029	6.0	45	45	10	200	75
1488	11.3	40	40	20	100	75
2184	12.9	30	30	40	100	75
3115	21	30	30	40	50	0
3551	24.6	40	40	20	50	0
3860	26.5	40	40	20	50	−50
4213	38	10	10	80	25	−100
5100	50	Basement			0	0
Baiyun Sag Pseudowell						
1230	0	50	40	10	1230	1230
2390	10.5	50	40	10	1750	250
2890	12.5	50	40	10	1750	250
3410	13.8	50	40	10	1750	250
3650	15.5	50	40	10	1750	250
4020	16.5	50	40	10	1750	250
4380	17.5	50	40	10	1750	250
5630	21	50	40	10	100	0
7700	30	50	40	10	100	0
10330	36	30	30	50	100	0
14350	45	Basement			0	0

finer grained than that found at Well 33-1-1. Compared to water depth uncertainties moderate changes in the relative proportions of silt to shale that dominate the backstripped sections are insignificant as a source of uncertainty to the subsidence analysis. Well 33-1-1 reached basement at a depth of 5104 m below sealevel and accumulated a sandstone-dominated Eocene section, followed by a silty–muddy section of Oligocene which is still of fluvial–lacustrine facies. Marine sedimentation started in the Miocene and remained dominated by clayey siltstone throughout. A deepening to outer shelf and then upper slope conditions occurred in the Late Miocene (Table 1).

Most conceptual models predict a slowing of subsidence after the end of active extension, but on the South China margin subsidence accelerated ~4 m.y. after the end of brittle extension. Our backstripping of the Baiyun Sag shows that subsidence was rapid after ~21–24 Ma (Fig. 3B). In particular, water depths rapidly increased from shallow shelf to bathyal (>250 m) in the Early Miocene (24 and 21 Ma) (Fig. 3B) (Pang et al., 2009). The basin developed an unconformity at ~24 Ma. Older Oligocene sedimentary rocks are interpreted to be of lacustrine facies, at least at Well 33-1-1, meaning that the central Baiyun Sag was likely not deeper than shelf depths until 24 Ma, after which a major change occurred. Fast post-rift subsidence after 21 Ma generated ~1200 m of anomalous subsidence in Baiyun Sag (Xie et al., 2014) despite the lack of any evidence for synchronous faulting (Fig. 2). Analysis of seismic profiles has also identified a late stage of faster subsidence at 17 to 11 Ma (Chen, 2014), although the degree of brittle extension seen on reflection profiles was minimal at that time (Sun et al., 2008).

Fig. 3B compares the reconstructed subsidence with two theoretical curves based on a uniform extension model (McKenzie, 1978) and the assumption that rapid extension finished at 30 Ma, at the onset of seafloor spreading. The total amount of syn-rift subsidence was used to predict the amount of post-rift, thermal subsidence. The observed subsidence is far in excess of the prediction after 21 Ma requiring additional tectonism to account for the basin depth.

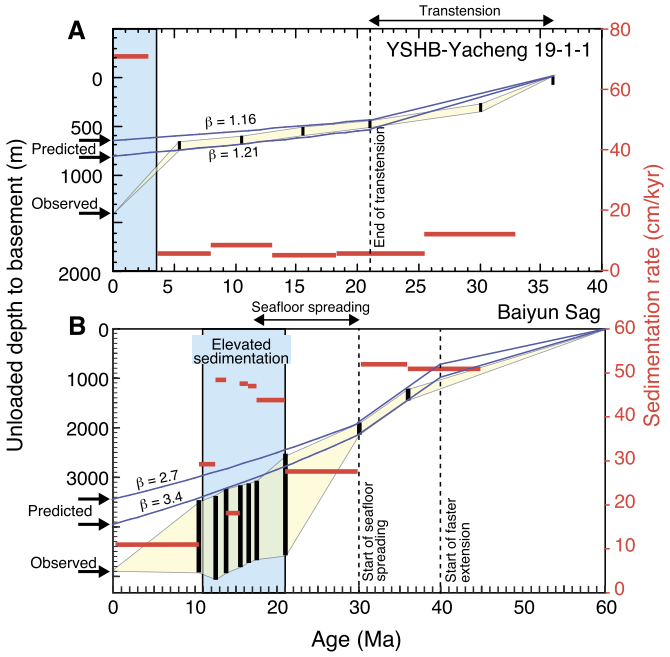

Fig. 3. Backstripped tectonic subsidence curve for two wells (A) Yacheng 19-1-1 in the YSHB (Clift and Sun, 2006), as well as (B) a pseudowell derived from seismic data and a nearby well from the Baiyun Sag. Vertical black bars indicate uncertainties in water depth of sedimentation, with yellow shading shows the range of basement depths through time. Each reconstruction is compared with maximum and minimum theoretical subsidence curves (dark blue) that are calculated from the amount of syn-rift subsidence. Arrows on the left of the figures show the modern day sediment unloaded depth to basement and the depth predicted from the syn-rift. (B) compares the Baiyun Sag with models with major extension ending at 30 Ma, at the start of seafloor spreading. Horizontal red bars indicate average rates of sedimentation and correspond to the scale on the right side of each figure. Light blue area shows timing of accelerated subsidence derived from regional seismic profiles (Chen, 2014).

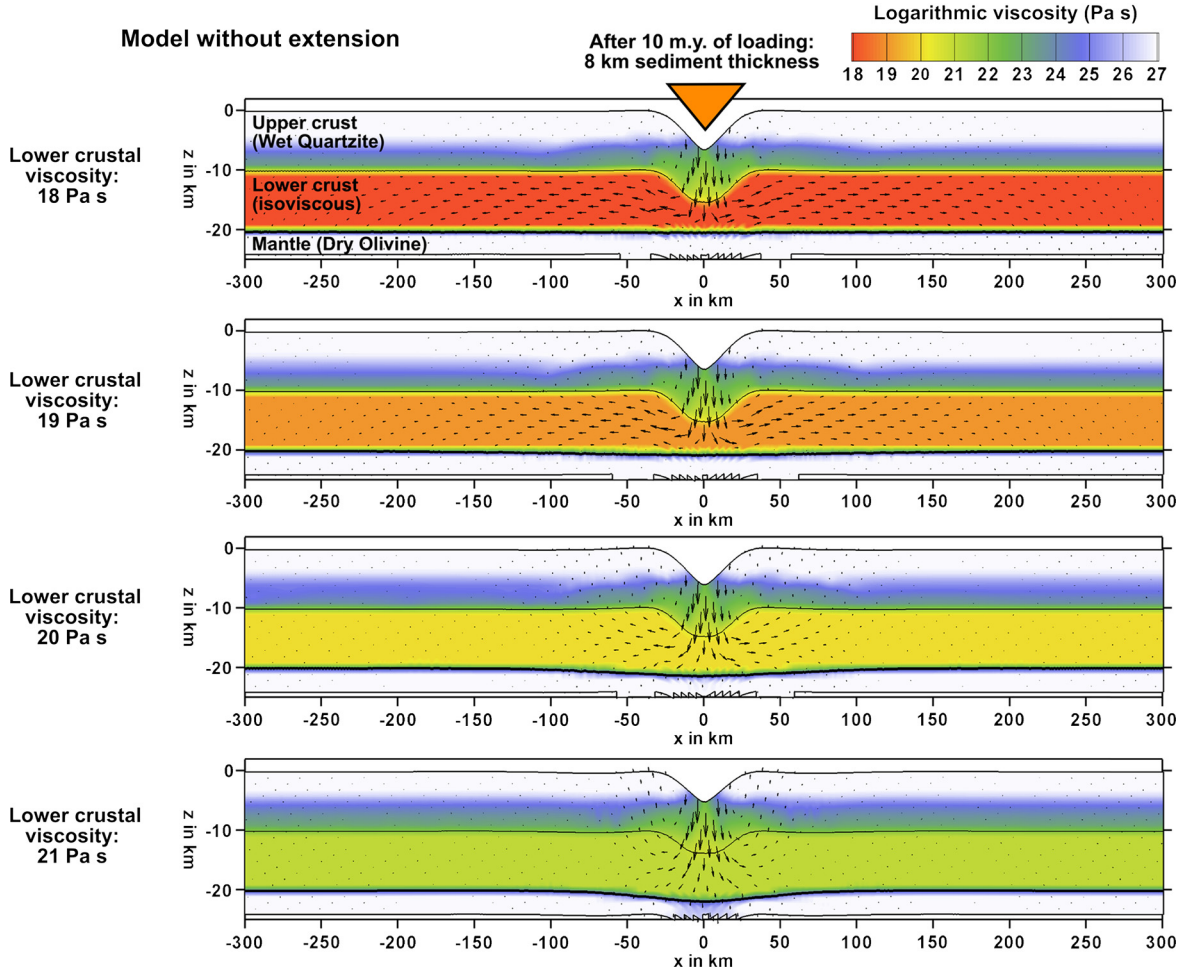

Fig. 4. Effect of lower crustal viscosity in the simplified model without extension. Images show crustal structure, logarithmic viscosities and material flow when the maximum sediment load is reached, 10 m.y. after sedimentation started. For weak lower crust, the load-induced vertical motion of the upper crust is translated to lower crustal flow, while for strong lower crust it leads to Moho subsidence. Lateral lower crustal flow can exceed 100 km if viscosity is sufficiently low.

4. Miocene climate change. Monsoon. Erosion and sedimentation

Here we argue that climatically modulated erosion is a viable mechanism for driving the sediment loading and crustal flow under the rifted margin during the Early and Middle Miocene. Although debate continues about the history of the East Asian Summer Monsoon, there is increasing evidence that initial intensification of this phenomenon began around the start of the Miocene, ~23 Ma. Changes in the flora of continental China (Sun and Wang, 2005) date from around this time and sedimentation rates across continental margins and deltas in South and SE Asia increased, as might be expected under the influence of heavier precipitation driving faster erosion in the source regions (Clift, 2006). Although it has been suggested that stronger monsoons might reduce erosion by encouraging greater vegetation growth (Castillo et al., 1997; Morgan, 2005) and that this in turn would impede erosion of soils, this reaction appears to mostly apply to semi-arid settings or mountain regions (Burbank et al., 2003), unlike the source regions of southern China. More recent evidence from modern river systems shows that precipitation is positively correlated with faster erosion and that this likely reflects the crucial role of rainfall in fostering landsliding, which is the most effective sediment producing process (Bookhagen et al., 2005). Recent analysis of the chemical weathering history in the South China Sea also supports increased weathering after ~23 Ma, consistent with an increase in humidity and seasonality under the influence of a strengthening monsoon (Clift et al., 2014; Wan et al., 2007). This monsoon is responsible for delivering extra sediment to the Pearl River offshore in the absence of major tectonic activity in the drainage basin at that time.

We discount tectonically driven rock uplift as a trigger for the faster erosion because active rifting is finished in the Pearl River Mouth Basin about around 25 Ma (Clift and Lin, 2001; Sun et al., 2008), so that the continental margin was a state of passive thermal subsidence at the time that the anomalous subsidence occurs. The headwater of the Pearl River today extend into the lower slopes of the Tibetan Plateau and there is evidence that some surface uplift was occurring in SW China at this time (Wang et al., 2012), which could be the trigger for an erosional pulse. However, drainage models for SE Asia suggest that the Pearl River basin was smaller than it is today at the time (Hoang et al., 2009) and since this pulse is something recognized in many basins across the region at this time (Clift, 2006), coincident with climate change, the most likely explanation for the faster sediment delivery is a climate trigger.

5. Numerical modeling

Using numerical forward modeling, we test under which circumstances monsoon induced sedimentation can lead to significant crustal thinning during the post-rift phase. This is accomplished using two model setups: a simple generic experiment (Fig. 4) and a more complex model setup accounting for the tectonic history of the South China Sea (Fig. 5). In both cases,

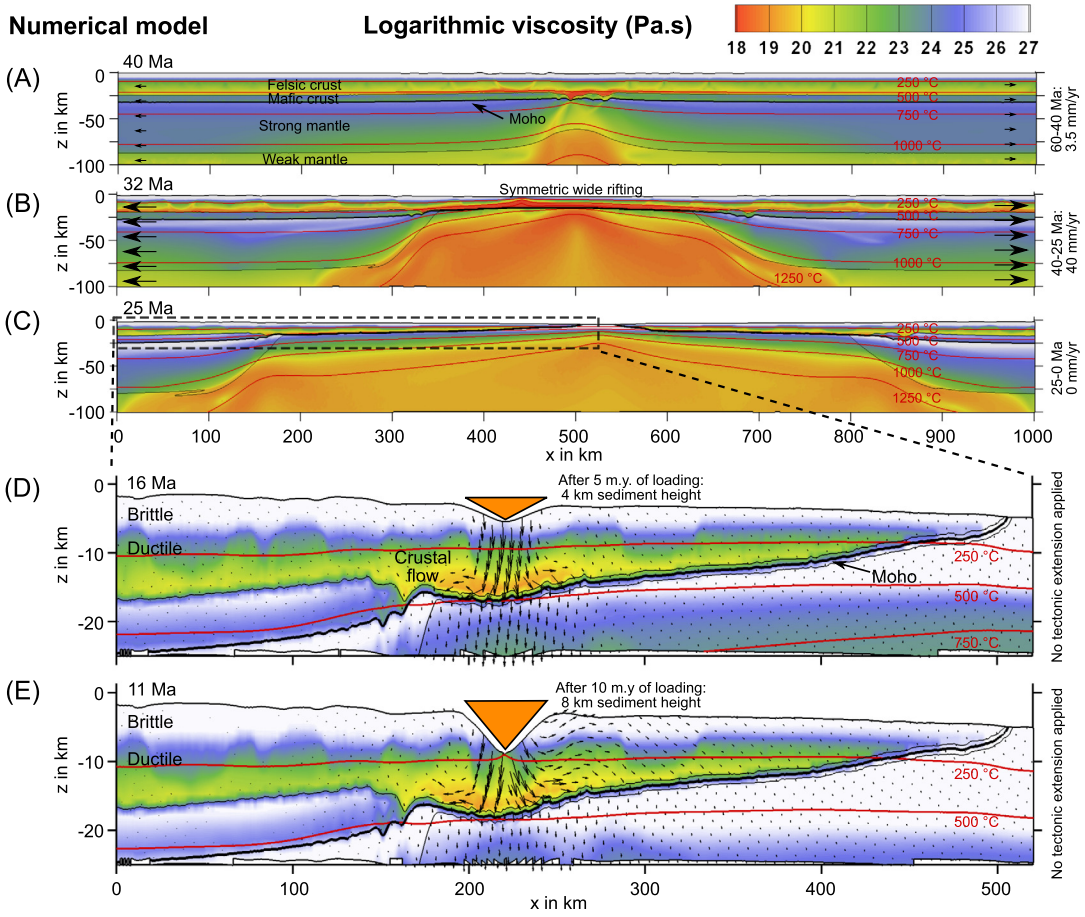

Fig. 5. Crustal structure, temperature, viscosity and direction of flow based on the numerical model as outlined in the text. Model has sediment loading starting at 21 Ma and increasing to full load until 11 Ma. Sediment distribution is indicated by orange triangle. (A)–(C) The weak crust decouples deformation of crust and mantle. A wide rift develops into two symmetric margins. (D)–(E) Post-breakup sediment loading is accommodated by lateral flow of the low-viscosity ($\sim 10^{19.5}$–10^{20} Pa s) crust.

we quantify how lower crustal flow accommodates strain in a sediment-loaded rifted margin setting. For simplicity, we approximate the sedimentation distribution of the Baiyun Sag basin through a triangular shape of 50 km width and 8 km height (orange triangle in Figs. 4 and 5). Assuming a constant sedimentation rate, the sediment thickness increases linearly from zero to 8 km within 10 m.y. Instead of introducing sediments as a proper material phase, we prescribe a local boundary stress corresponding to the triangular sediment distribution. This procedure robustly incorporates the effect of a space- and time-dependent sediment load on the crystalline basement, even though the internal structure of the sediments is not resolved. We account for thermal insulation of the sediments by correlating model surface temperature with sediment thickness through a constant thermal gradient of 30 °C/km, which yields a final peak temperature of 250 °C at the bottom of the basin.

The applied numerical finite-element code is a two-dimensional version of the thermo-mechanical forward modeling software SLIM3D (Popov and Sobolev, 2008). The elasto–visco–plastic model allows to address a wide range of rift-related deformation processes such as flexure, lower crustal flow, and faulting (Brune, 2014; Brune et al., 2014). Details on the numerical, thermal, and rheological setup including all model parameters are given in the Supporting Information.

First we conduct a simple experiment without extension. A laterally homogeneous lithosphere with two crustal and a mantle layer is exposed to the aforementioned time-dependent sediment load. The lower crust has a prescribed viscosity while the upper crustal and mantle layer deform via a laboratory-derived wet quartzite and dry olivine flow law involving temperature- and stress-dependent viscosity. Fig. 4 shows the flow field of four models with different lower crustal viscosities of 18 to 21 Pa s after 10 m.y. of continuous sedimentation. For the weakest lower crust (10^{18} Pa s), all vertical surface motion is compensated by lower crustal flow. The Moho discontinuity remains flat and no elastic bulge occurs adjacent to the load. In this model the distance at which lateral crustal flow takes place is limited by the left and right model boundary. For a crustal viscosity of 10^{19} Pa s, the result is nearly identical. Note that analytical estimates of crustal viscosity in the South China Sea (Clift et al., 2002) based on regional slope range between 10^{18} and 10^{19} Pa s. With a viscosity of 10^{20} Pa s, lateral flow occurs within a distance of about 75 km to each side of the load. Within the same distance, a small amount of Moho subsidence can be observed. For a high viscosity of 10^{21} Pa s, lateral flow does not exceed 50 km distance from the load center and is compensated by Moho subsidence. Additionally, upward directed flow occurs throughout the crust in close proximity to the loading area leading to surface uplift.

We extend the previous model accounting for the tectonic environment of the South China Sea and by using temperature- and stress-dependent viscosity in all layers. In order to reproduce the time-dependent structure of the northern margin of the South China Sea we model the entire rift process by applying extensional velocities at the lateral boundaries of an initially layered setup. Based on a recent plate tectonic reconstruction (Zahirovic et al., 2014), we approximate the kinematic evolution of the South China Sea extension in a three-stage history: (i) Full extension velocities of 3.5 mm/yr between 60 Ma and 40 Ma, (ii) 40 mm/yr

between 40 Ma and 25 Ma, and (iii) after 25 Ma, the rifted margin remains without extension, although we recognize that there has been small degrees of extension of the shelf since that time (Lüdmann and Wong, 1999). Ongoing debate about the timing of seafloor spreading (Chang et al., 2015) do not affect the mode because all model agree that the passive margin was in a state of passive subsidence at the point and our model is not sensitive to the rate of seafloor spreading in the basin center at this time. The initial configuration has a 25-km-thick felsic upper crust, an 8-km-thick mafic lower crust, a sub-continental lithospheric mantle that extends down to 90 km and weak asthenospheric mantle below. Sediment loading starts at 21 Ma and increases linearly to full load until 11 Ma.

The model reproduces wide rifting where felsic crustal viscosities as low as 10^{18} Pa s decouple crust and mantle deformation, which ultimately generates two wide, symmetric margins with low topographic gradients, such as observed in this region (Clift et al., 2002). Enhanced sediment loading reminiscent of the Baiyun Sag basin (orange triangle in Fig. 5) commences during the post-rift phase. At this time, self-consistently evolving viscosities in the area of sedimentation range between $10^{19.5}$ Pa s and 10^{20} Pa s. In agreement with the simplified model set-up presented above, lateral flow occurs within a distance of more than 50 km from the loading site. This flow effectively thins the crust and compensates the surface subsidence with only minor Moho deflection.

6. Role of crustal flow

Although there is common understanding that post-rift subsidence acceleration has occurred in the South China Sea, there is little agreement about what caused this. Some have suggested that subsidence could be caused by emplacement of a dense intrusive body into the lower crust at ~17 Ma (Shi et al., 2005; Xie et al., 2006), followed by thermal cooling. However, magmatic thickening of crust results in uplift rather than subsidence, e.g., North Atlantic Tertiary (Brodie and White, 1994). Only if gabbroic melt is trapped at >50 km in the lithosphere and eclogitized then it may have potential to drive local subsidence (Hall and White, 1994). In any case no strong evidence exists to support intrusive magmatism into the base of the Baiyun Sag at 17 Ma, beyond some poorly defined seismic reflections in the lower crust in that region, but precisely what these represent is unknown.

Our finite element model indicates that rapid subsidence after 21 Ma reflects the influence of ductile flow in the post-rift period. As with the Plio-Pleistocene in the YSHB, the Early Miocene in the South China Sea is associated with faster sediment delivery to offshore basins (Clift, 2006; Xie et al., 2013) driven by a change to a more erosive, monsoonal climate around that time (Clift et al., 2014; Sun and Wang, 2005). In the Malay Basin a combination of onshore erosion and offshore sedimentation resulted in a reverse flow of ductile lower crust away from the basin center and toward the continental margin after the end of extension (Morley and Westaway, 2006). This requires the flow of crust towards regions of thicker crust, which is only explicable when understood as a readjustment from one state of stability (with thick crust under the margin and thin sediment offshore) to another (with thinner crust onshore and a thicker sediment load offshore). Removal of rock from onshore by erosion results in isostatic uplift, while at the same time increasing loads in the offshore act to change the pressure gradient across the coast, driving ductile material away from the basin axis and towards the continental interior. Net flow is still from thick to thin crustal regions achieved during active extension.

This process may be understood by considering where isostatic equilibrium is achieved. Mid crustal viscosity estimates based on the regional slope on the margin basement range from 10^{19} to 10^{18} Pa s within a hypothetical 5 km-wide mid crustal channel (Clift et al., 2002). While the lithosphere is generally estimated to have a viscosity of 10^{23} Pa s, the asthenosphere can have values of 10^{19} Pa s or lower, depending on water contents and temperature (Doglioni et al., 2011). These values overlap with those from the lower crust in South China and raise the possibility that loads on the continental margin might be compensated within the crust rather than on the lithospheric scale. We argue, based on the finite element modeling that loading of the continental margin during the Early Miocene drove the flow of ductile crust away from the basin axis, largely northwards under the Chinese margin, as first argued by Westaway (1994). Southward flow is impossible because the southern edge of Baiyun Sag abuts the oceanic, and therefore rigid, crust of the deep South China Sea.

Lateral crustal flow is a consequence of the weakness of the crust, caused by high heatflow, a weak quartz-rheology and is triggered by sediment loading. This type of deformation would not be anticipated in rifted margins where heatflow was low or little sedimentation was occurring. This is a new form of climate–tectonic interaction in which weak crust affected by extension can continue to deform and flow in the post-rift period as a result of changing erosion rates on the basin flanks delivering increased sediment loads to the basin center and altering the crustal structure offshore. We suggest that super-deep rift basins, like Baiyun Sag, are likely often linked to the flow of ductile crust in this fashion and would not be expected in cooler rift settings, such as found along the Atlantic margins.

7. Conclusions

Subsidence anomalies have been identified on continental margins in different parts of the world and of different ages, yet those of the South China Sea are of especially large magnitude and cannot be linked to many of the common cited processes, such as magmatic underplating or mantle circulation. We propose that flow of ductile mid and lower crust, inherited from an earlier phase of active margin magmatism, is the cause of this subsidence. While this crust flows towards the rift axis during break-up, causing an earlier phase of excess subsidence compared to the amount of brittle faulting, the flow reverses during the Early Miocene as a strengthening summer monsoon increased continental erosion and rapidly loaded the deep sub-basins on the margin with several kilometers of material. Numerical modeling shows that emplacement of such a load has the potential to drive flow away from the basin center and decrease the thickness of crystalline crust in the offshore. This is a newly recognized form of climate–tectonic interaction that might be recognized in any thermally juvenile continental margin that is subject to a strong erosional flux. Since monsoon-modulated erosion increased across the whole of SE Asia in the Early Miocene such subsidence pulses may be predicted in other Asian marginal basins at the same time, where sedimentation rates spike (Clift, 2006). This not only has implications for crustal structure in rifted margins but also for hydrocarbon exploration because simple measurement of extension factor based on modern basement depths will provide an inappropriate model of the thermal evolution.

Acknowledgements

P.C. thanks Chris Morley for discussing these topics and for support from the Charles T. McCord chair at LSU. S.B. has been funded by the European Research Council, Marie Curie International Outgoing Fellowship (Project 326115) and by SAMPLE (South Atlantic Margin Processes and Links with onshore Evolution), the German Research Foundation Priority Program 1375. J.Q. has been partially

funded by the Helmholtz Association as Head of a Helmholtz International Research Group (HIRG-008).

Appendix A. Supplementary material

Supplementary material related to this article can be found online at http://dx.doi.org/10.1016/j.epsl.2015.03.032.

References

Barckhausen, U., Engels, M., Franke, D., Ladage, S., Pubellier, M., 2014. Evolution of the South China sea: revised ages for breakup and seafloor spreading. Mar. Pet. Geol. http://dx.doi.org/10.1016/j.marpetgeo.2014.02.022.

Block, L., Royden, L.H., 1990. Core complex geometries and regional scale flow in the lower crust. Tectonics 9, 557–567.

Bookhagen, B., Thiede, R.C., Strecker, M.R., 2005. Late quaternary intensified monsoon phases control landscape evolution in the northwest Himalaya. Geology 33 (2), 149–152.

Briais, A., Patriat, P., Tapponnier, P., 1993. Updated interpretation of magnetic anomalies and seafloor spreading stages in the South China Sea: implications for the Tertiary tectonics of Southeast Asia. J. Geophys. Res. 98, 6299–6328.

Brodie, J., White, N., 1994. Sedimentary basin inversion caused by igneous underplating: Northwest European continental shelf. Geology 22, 147–150.

Brune, S., 2014. Evolution of stress and fault patterns in oblique rift systems: 3-D numerical lithospheric-scale experiments from rift to breakup. Geochem. Geophys. Geosyst. 15, 3392–3415.

Brune, S., Heine, C., Perez-Gussinye, M., Sobolev, S.V., 2014. Rift migration explains continental margin asymmetry and crustal hyper-extension. Nat. Commun. 5 (4014). http://dx.doi.org/10.1038/ncomms5014.

Burbank, D.W., Blythe, A.E., Putkonen, J., Pratt-Sitaula, B., Gabet, E., Oskins, M., Barros, A., Ojha, T.P., 2003. Decoupling of erosion and precipitation in the Himalayas. Nature 426, 652–655.

Castillo, V.M., Martinez-Mena, M., Albaladejo, J., 1997. Runoff and soil loss response to vegetation removal in a semiarid environment. Soil Sci. Soc. Am. J. 61, 1116–1121.

Chang, J.-H., Lee, T.-Y., Hsu, H.-H., Liu, C.-S., 2015. Comment on Barckhausen et al., 2014 – Evolution of the South China Sea: revised ages for breakup and seafloor spreading. Mar. Pet. Geol. 59, 676–678.

Chen, L., 2014. Stretching factor estimation for the long-duration and multi-stage continental extensional tectonics: application to the Baiyun Sag in the northern margin of the South China Sea. Tectonophysics 611, 167–180.

Clark, M.K., Royden, L.H., 2000. Topographic ooze: building the eastern margin of Tibet by lower crustal flow. Geology 28, 703–706.

Clift, P., Lin, J., 2001. Preferential mantle lithospheric extension under the South China margin. Mar. Pet. Geol. 18 (8), 929–945.

Clift, P., Lin, J., Barckhausen, U., 2002. Evidence of low flexural rigidity and low viscosity lower continental crust during continental break-up in the South China Sea. Mar. Pet. Geol. 19 (8), 951–970.

Clift, P.D., 2006. Controls on the erosion of Cenozoic Asia and the flux of clastic sediment to the ocean. Earth Planet. Sci. Lett. 241 (3–4), 571–580.

Clift, P.D., Sun, Z., 2006. The sedimentary and tectonic evolution of the Yinggehai–Song Hong Basin and the southern Hainan margin, South China Sea; implications for Tibetan uplift and monsoon intensification. J. Geophys. Res. 111 (B6), 28.

Clift, P.D., Wan, S., Blusztajn, J., 2014. Reconstructing chemical weathering, physical erosion and monsoon intensity since 25 Ma in the northern South China Sea: a review of competing proxies. Earth-Sci. Rev. 130, 86–102.

Davis, M., Kusznir, N.J., 2004. Depth-dependent lithospheric stretching at rifted continental margins. In: Karner, G.D. (Ed.), Proceedings of NSF Rifted Margins Theoretical Institute. Columbia University Press, New York, pp. 92–136.

Doglioni, C., Ismail-Zadeh, A., Panza, G., Riguzzi, F., 2011. Lithosphere–asthenosphere viscosity constrast and decoupling. Phys. Earth Planet. Inter. 189 (1–2), 1–8.

Franke, D., Savva, D., Pubellier, M., Steuer, S., Mouly, B., Auxietre, J.-L., Meresse, F., Chamot-Rooke, N., 2014. The final rifting evolution in the South China Sea. Mar. Pet. Geol. 58B, 704–720. http://dx.doi.org/10.1016/j.marpetgeo.2013.11.020.

Hall, B.D., White, N., 1994. Origin of anomalous Tertiary subsidence adjacent to North Atlantic continental margins. Mar. Pet. Geol. 11 (6), 702–714.

Hoang, L.V., Wu, F.Y., Clift, P.D., Wysocka, A., Swierczewska, A., 2009. Evaluating the evolution of the Red River system based on in-situ U–Pb dating and Hf isotope analysis of zircons. Geochem. Geophys. Geosyst. 10, Q11008.

Kruse, S., McNutt, M.K., Phipps-Morgan, J., Royden, L., Wernicke, B.P., 1991. Lithospheric extension near Lake Mead, Nevada; a model for ductile flow in the lower crust. J. Geophys. Res. 96 (3), 4435–4456.

Lithgow-Bertelloni, C., Gurnis, M., 1997. Cenozoic subsidence and uplift of continents from time-varying dynamic topography. Geology 25, 735–738.

Lüdmann, T., Wong, H.K., 1999. Neotectonic regime on the passive continental margin of the northern South China Sea. Tectonophysics 311, 113–138.

McKenzie, D.P., 1978. Some remarks on the development of sedimentary basins. Earth Planet. Sci. Lett. 40, 25–32.

Morgan, R.P.C., 2005. Soil Erosion and Conservation. Blackwell, Oxford. 325 pp.

Morley, C.K., 2002. A tectonic model for the Tertiary evolution of strike-slip faults and rift basins in SE Asia. Tectonophysics 347 (4), 189–215.

Morley, C.K., Westaway, R., 2006. Subsidence in the super-deep Pattani and Malay basins of Southeast Asia: a coupled model incorporating lower-crustal flow in response to post-rift sediment loading. Basin Res. 18, 51–84.

Morley, C.K., 2012. Late Cretaceous–Early Palaeogene tectonic development of SE Asia. Earth-Sci. Rev. 115 (1), 37–75.

Pang, X., Chen, C., Zhu, M., He, M., Shen, J., Lian, S., Wu, X., Shao, L., 2009. Baiyun movement: a significant tectonic event on Oligocene/Miocene boundary in the Northern South China Sea and its regional implications. J. Earth Sci. 20 (1), 49–56.

Peltzer, G., Tapponnier, P., 1988. Formation and evolution of strike-slip faults, rifts, and basins during the India–Asia Collision: an experimental approach. J. Geophys. Res. 93, 15085–15117.

Petersen, K.D., Nielsen, S.B., Clausen, O.R., Stephenson, R., Gerya, T., 2010. Small-scale mantle convection produces stratigraphic sequences in sedimentary basins. Science 329, 827–830.

Popov, A.A., Sobolev, S.V., 2008. SLIM3D: a tool for three-dimensional thermo mechanical modeling of lithospheric deformation with elasto–visco–plastic rheology. Phys. Earth Planet. Inter. 171, 55–75.

Sclater, J.G., Christie, P.A.F., 1980. Continental stretching: an explanation of the post Mid-Cretaceous subsidence of the central North Sea basin. J. Geophys. Res. 85, 3711–3739.

Shi, X., Burov, E., Leroy, S., Qiu, X., Xia, B., 2005. Intrusion and its implication for subsidence: a case from the Baiyun Sag, on the northern margin of the South China Sea. Tectonophysics 407 (1–2), 117–134.

Sun, X., Wang, P., 2005. How old is the Asian monsoon system? Palaeobotanical records from China. Palaeogeogr. Palaeoclimatol. Palaeoecol. 222 (3–4), 181–222.

Sun, Z., Zhong, Z., Zhou, D., Pang, X., Huang, C.C., Chen, C., He, M., Xu, H., 2008. Dynamics analysis of the Baiyun Sag in the Pearl River Mouth Basin. North of the South China Sea. Acta Geol. Sin. 82 (1), 73–83.

Taylor, B., Hayes, D.E., 1983. Origin and history of the South China Sea basin. In: Hayes, D.E. (Ed.), The Tectonic and Geologic Evolution of the Southeast Asian Seas and Islands. American Geophysical Union, Washington, DC, pp. 23–56.

Wan, S., Li, A., Clift, P.D., Stuut, J.-B.W., 2007. Development of the East Asian monsoon: mineralogical and sedimentologic records in the northern South China Sea since 20 Ma. Palaeogeogr. Palaeoclimatol. Palaeoecol. 254 (3–4), 561–582.

Wang, E., Kirby, E., Furlong, K.P., Soest, M.v., Xu, G., Shi, X., Kamp, P.J.J., Hodges, K.V., 2012. Two-phase growth of high topography in eastern Tibet during the Cenozoic. Nat. Geosci. 5, 640–645.

Wernicke, B.P., 1990. The fluid crustal layer and its implications for continental dynamics. In: Salisbury, M.H., Fountain, D.M. (Eds.), Exposed Cross-Sections of the Continental Crust. In: NATO ASI Series. Kluwer Academic Publishers, Dordrecht, The Netherlands, pp. 509–544.

Westaway, R., 1994. Re-evaluation of extension across the Pearl River Mouth Basin, South China Sea: implications for continental lithosphere deformation mechanisms. J. Struct. Geol. 16, 823–838.

Wheeler, P., White, N., 2002. Measuring dynamic topography: an analysis of Southeast Asia. Tectonics 21 (5), 1040.

Xie, X.N., Müller, R.D., Li, S.T., Gong, Z.S., Steinberger, B., 2006. Origin of anomalous subsidence along the Northern South China Sea margin and its relationship to dynamic topography. Mar. Pet. Geol. 23 (7), 745–765.

Xie, H., Zhou, D., Pang, X., Li, Y., Wu, X., Qiu, N., Li, P., Chen, G., 2013. Cenozoic sedimentary evolution of deepwater sags in the Pearl River Mouth Basin, northern South China Sea. Mar. Geophys. Res. 34, 159–173. http://dx.doi.org/10.1007/s11001-013-9183-7.

Xie, H., Zhou, D., Li, Y., Pang, X., Li, P., Chen, G., Li, F., Cao, J., 2014. Cenozoic tectonic subsidence in deepwater sags in the Pearl River Mouth Basin, northern South China Sea. Tectonophysics 615–616, 182–198.

Zahirovic, S., Seton, M., Müller, R.D., 2014. The Cretaceous and Cenozoic tectonic evolution of Southeast Asia. Solid Earth Discuss. 5, 227–273.

Zhao, Z.X., Sun, Z., Xie, H., Yan, C.Z., Li, Y.P., 2011. Cenozoic subsidence and lithospheric stretching deformation of the Baiyun deepwater area. Chin. J. Geophys. 54 (6), 1159–1166.

Zuber, M.T., Parmentier, E.M., Fletcher, R.C., 1986. Extension of continental lithosphere: a model for two scales of basin and range deformation. J. Geophys. Res. 91, 4826–4838.